Weather and Climate Extremes 43 (2024) 100649

Contents lists available at ScienceDirect

Weather and Climate Extremes

journal homepage: www.elsevier.com/locate/wace

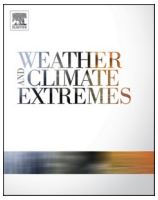

Air-sea coupling influence on projected changes in major Atlantic hurricane events

Derrick K. Danso [a,*], Christina M. Patricola [a,b], Jaison Kurian [c], Ping Chang [c], Philip Klotzbach [d], I.-I. Lin [e]

[a] Department of Geological and Atmospheric Sciences, Iowa State University, Ames, USA
[b] Climate and Ecosystem Sciences Division, Lawrence Berkeley National Laboratory, Berkeley, CA, USA
[c] Department of Oceanography, Texas A&M University, College Station, TX, USA
[d] Department of Atmospheric Science, Colorado State University, Fort Collins, CO, USA
[e] Department of Atmospheric Sciences, National Taiwan University, Taipei, Taiwan

A B S T R A C T

Tropical cyclone (TC) projections with atmosphere-only models are associated with uncertainties due to their inability to represent TC-ocean interactions. However, global coupled models, which represent TC-ocean interactions, can produce basin-scale sea surface temperature biases in seasonal to centennial simulations that lead to challenges in representing TC activity. Therefore, focusing on recent individual major hurricane events, we investigated the influence of TC-ocean coupling on the response of TCs to anthropogenic change using atmosphere-only and coupled atmosphere-ocean regional model simulations. Under an extremely warm scenario, coupling does not influence the signs of projected TC rainfall and intensity responses. Coupling, however, does influence the magnitude of projected intensity and especially rainfall. Within a 500 km radius region of the TCs, the projected rainfall increases in coupled simulations are 3–59 % less than in the atmosphere-only simulations, driven by enhanced TC-induced sea surface temperature cooling in the former. However, the influence of coupling on the magnitude of projected rainfall could vary considerably over the regions of highest rainfall generated by TCs.

1. Introduction

One of the most significant natural disasters is tropical cyclones (TC) due to their damaging and deadly impacts on human life and infrastructure. Globally, North Atlantic (hereafter Atlantic) TCs have led to the largest economic losses, with the four costliest hurricanes on record—Katrina, Harvey, Ian, and Maria—leading to 190, 151, 113, and 109 billion US dollars losses, respectively (NOAA National Centers for Environmental Information (NCEI), 2023). There is no consensus on how anthropogenic warming will change TC frequency in the future (e.g., Knutson et al., 2020; Walsh et al., 2016). However, recent observations have shown that TC rainfall and intensity in the North Atlantic has increased (Bhatia et al., 2019; Klotzbach, 2006; Lau and Zhou, 2012). Numerical modeling studies have suggested that anthropogenic warming is responsible for the enhanced rainfall and intensity of several recent major TCs (Patricola and Wehner, 2018; Reed et al., 2020). Therefore, economic damages associated with TCs may substantially increase in the future due to projected global warming (Grinsted et al., 2013; Knutson et al., 2015). Reliable future projections of TC activity are thus necessary to improve the preparedness and resilience of affected regions.

However, projections of TC activity under future climates are characterized by many uncertainties. For example, atmosphere-only global climate models (GCM) used for simulating TCs in the current and future climates do not represent TC-ocean interactions due to the use of prescribed sea surface temperatures (SST). It is well known that strong near-surface TC winds can induce SST cooling commonly referred to as cold wakes (e.g., Chen et al., 2017; Kuttippurath et al., 2022; Pasquero et al., 2021; Price, 1981; Zhang et al., 2019). TC winds induce cold wakes by vertically mixing the upper ocean and enhancing cold water upwelling from below the ocean surface (Lu et al., 2021; Vincent et al., 2012). This process can significantly reduce the ocean surface enthalpy flux which may in turn, weaken TCs (Emanuel, 1999; Guo et al., 2020; Karnauskas et al., 2021; Walker et al., 2014). The rate of this feedback depends on upper ocean characteristics including stratification, heat content, and salinity (Balaguru et al., 2012; Huang et al., 2015; Zhang et al., 2021b). It also depends on the depth of the 26 °C subsurface isotherm which can modify TC-induced cooling (Lin et al., 2008). The strength of TC-induced cooling is also influenced by TC characteristics including intensity, size, and translation speed (Mei et al. 2012, 2015a; Pun et al.,

* Corresponding author.
E-mail address: ddanso@iastate.edu (D.K. Danso).

https://doi.org/10.1016/j.wace.2024.100649
Received 25 August 2023; Received in revised form 24 January 2024; Accepted 29 January 2024
Available online 30 January 2024

2021). The influence of translation speed on TC-induced cooling further depends on the depth and heat content of the subsurface layer (Lin et al., 2009).

These complex interactions, all of which could be modified under climate change (Emanuel, 2021; Schwinger et al., 2014), are better represented in coupled simulations in which TCs and the ocean interact (Mogensen et al., 2017). This therefore makes coupled GCMs important tools in the projection and understanding of future TC activity in a changing climate. For instance, coupled GCM projections have shown that TC precipitation will increase in most regions; however, the magnitude can vary greatly depending on ocean coupling (Huang et al., 2021). Nevertheless, coupled GCM simulations which are usually focused on seasonal to centennial predictions of TCs are characterized by large basin-scale SST biases (Richter, 2015; Zuidema et al., 2016), which can impact the representation of TCs in the models. This can introduce systematic biases and uncertainties in projected future TC statistics (Dutheil et al., 2020; Hsu et al., 2019; Huang et al., 2021; Zhang et al., 2021a). Given the differences between coupled and uncoupled simulations of TC activity (Li and Sriver, 2018, 2019; Srinivas et al., 2016; Zarzycki, 2016), precisely characterizing the influence of TC-ocean coupling on projections of future TC activity remains challenging. The basin-scale SST biases typically produced by long term GCM simulations may be minimized however, by focusing on single TC events that typically last up to a few weeks.

Therefore, the main objective of this study is to quantify the influence of TC-ocean coupling on projections of several recent major Atlantic TC events using regional model simulations. We investigate how some of the most impactful recent TC events will change in future warmer climates, with numerical simulations using an atmosphere-only model and a coupled model. The event-based simulations are designed to minimize basin-scale SST biases typical of coupled simulations lasting more than a few weeks. Although previous studies (e.g., Patricola and Wehner (2018) and Reed et al. (2020)) have simulated single TC events, they did not investigate the impact of TC-ocean interactions. Thus, the main novelty here is using a coupled atmosphere-ocean model to simulate multiple hurricanes in a single basin. We further explore whether the influence of TC-ocean coupling on simulated statistics will be modified in a future warmer climate relative to historical conditions.

2. Methods and models

2.1. Description of atmosphere-only and coupled models

Simulations of TC events were performed using the Coupled Ocean–Atmosphere–Wave–Sediment Transport (COAWST) modeling system (Warner et al., 2010) version 3.7. COAWST consists of multiple sophisticated tools used for modeling different components of the earth system including the atmosphere, ocean, ocean waves, hydrology, and coastal sediment transport. For this study, we only used the atmosphere and ocean models. TC simulations were performed with the Weather Research and Forecasting (WRF) model version 4.2.2 (Skamarock et al., 2019) and the Regional Ocean Modeling System (ROMS) version 3.9 (Haidvogel et al., 2008; Shchepetkin and McWilliams, 2005). The COAWST system is well suited for this study for two main reasons. First, it can be configured to actively exchange fields between different components by coupling two or more models. The exchange of fields is performed using the Model Coupling Toolkit (MCT) version 2.6.0 (Jacob et al., 2005; Larson et al., 2005). Second, each model can also be run independently of the others.

The WRF model was configured with a 12 km horizontal resolution and 45 vertical levels. This horizontal resolution is sufficient for this study as shown by Patricola and Wehner (2018), who found that WRF simulations with horizontal resolution between 3 km and 27 km did not introduce a substantial uncertainty in the sign of the projected statistics. Initial and lateral boundary conditions and SST were prescribed from the fifth-generation European Centre for Medium-Range Weather Forecasts (ECMWF) Reanalysis (ERA5) (Hersbach et al., 2020). Convection in the simulations was parameterized with the Kain-Fritsch scheme (Kain, 2004). The ROMS was also configured with a 12 km horizontal resolution. The model uses a free surface, terrain-following vertical sigma coordinates to solve the Reynolds-averaged Navier Stokes equation assuming hydrostatic equilibrium and Boussinesq approximations (Shchepetkin and McWilliams, 2005). For this study, it was configured with 40 sigma levels for the terrain-following vertical layers. With a critical depth of 250 m, the surface and bottom stretching parameters were set as 10 and 0.1, respectively, to control the stretching and default vertical coordinate transformation. The initial and open boundary conditions of temperature, salinity, current velocities, and sea surface height were obtained from the global Hybrid Coordinate Ocean Model (HYCOM) with Naval Research Lab (NRL) Coupled Ocean Data Assimilation (NCODA) 1/12° reanalysis, which assimilates satellite and in-situ observations (Chassignet et al., 2009). In the atmosphere-only simulations, WRF is run alone and does not exchange fields with ROMS. In the coupled atmosphere-ocean simulations, however, SST is passed from ROMS to WRF, while ROMS receives sea surface stresses and net heat fluxes from WRF. The atmosphere and ocean models exchange flux information at a time interval of 10 minutes. It should be noted that SST cold wakes may still exist in the atmosphere-only simulations, despite lacking active air-sea coupling. This is due to using prescribed SSTs for the atmosphere-only simulations from ERA5. Since SST in ERA5 is based on observed data from satellites and other instruments, SST cold wakes may already exist in the reanalysis. However, active coupling between the atmosphere and ocean is not activated.

2.2. Historical TC event simulations

We first performed atmosphere-only (WRF) historical control simulations of six recent impactful TCs, including four of the ten costliest Atlantic TCs on record (i.e., Hurricanes Ida (2021), Irma (2017), Maria (2017), and Michael (2018)), as well as Arthur (2014) and Nate (2017) (Supplementary Table 1). These simulations represent hindcasts of the actual conditions in which the TC events occurred. The selected TCs reached hurricane or major hurricane status and affected areas such as the Gulf Coast, Florida, the mid-Atlantic coast, and the Caribbean islands. The prescribed ERA5 initial and boundary conditions were used for the historical control simulations without any adjustments. For each simulated TC, the model initialization time was chosen to account for much of the TC's lifetime while also being able to realistically represent the observed TC's evolution, especially its track. This is because previous studies (Patricola and Wehner, 2018) have shown that earlier initialization times produced larger deviations between simulated and actual TC tracks. The initialization times used to obtain the best tracks for the simulated TCs are provided in Supplementary Table 1. The TC intensity in the atmosphere-only model was spun up from the initial conditions within a few hours. Ten ensemble members were generated for each TC simulation using the same model initialization time and initial and boundary conditions but with different planetary boundary layers or microphysics schemes in the WRF model as done in previous studies (e.g., Lackmann (2015)).

We then performed historical simulations consisting of coupled atmosphere-ocean (WRF and ROMS) hindcasts of the same TCs. In the coupled simulations, the atmosphere model configuration was the same as used in the atmosphere-only hindcasts, while the initial and boundary conditions prescribed from HYCOM were used in the ocean model. Like the atmosphere-only simulations, the TC intensity in the coupled model spun up from the initial conditions within a few hours. Simulation domains varied for the different TCs, but their construction followed a similar convention. The longitude and latitude bounds of both the atmosphere and ocean grids for all of the TCs are shown in Supplementary Table 1. In the coupled simulations, the ROMS domain was constructed such that it covered most of the TC's lifetime over the ocean. It was nested within a larger WRF domain, which was also used for

atmosphere-only simulations. This convention helped to minimize the potential influence of WRF's lateral edge effects on the ocean. Fig. 1 shows the model domains used to simulate TCs that affected the Gulf Coast.

2.3. Pseudo-global warming experiments

With both the uncoupled and coupled configurations, we then performed pseudo-global warming (PGW) experiments (Schär et al., 1996) representing the selected TCs if they were to occur at the end of the 21st century in extremely warm conditions. This PGW method has been used in many studies to identify current and future anthropogenic influences on extreme events (e.g., Lackmann, 2015; Pall et al., 2017; Patricola and Wehner, 2018; Reed et al., 2020). The initial and lateral boundary conditions for the PGW experiments were those from the historical simulations, adjusted with spatially-varying perturbations representing the thermodynamic component of anthropogenic climate change. The perturbation for the end of the 21st century was estimated from the Energy Exascale Earth System Model (E3SM) version 1 (Golaz et al., 2019) based on the Shared Socioeconomic Pathway (Riahi et al., 2017) SSP5-8.5 high-end warming scenario of the Coupled Model Intercomparison Project phase 6 (CMIP6) (Eyring et al., 2016).

For each of the selected TCs, the perturbation was calculated using the climatological mean for the month in which the TC occurred based on a 100-year difference between the future SSP5-8.5 scenario and historical period. For example, the perturbation for Hurricane Irma and Maria was calculated as the difference between the September climatology at the end of the 21st century (2080–2100) from SSP5-8.5 and 20th century (1980–2000) historical simulations of E3SM. We did not test the sensitivity of the anthropogenic TC response to the selected periods. The historical initial and boundary conditions used for both the atmosphere-only and coupled models were then adjusted by adding the computed climate change perturbations.

The following variables in the initial and boundary conditions were adjusted in the atmosphere-only simulations: surface temperature, air temperature, relative humidity, land and sea surface temperature, surface pressure, sea level pressure, atmospheric pressure, soil temperature, and geopotential height. We also modified the concentrations of greenhouse gases, including CO2, N2O, CH4, CCl4, CFC-11, and CFC-12, based on the official anthropogenic emissions used for the CMIP6 project in the SSP5-8.5 scenario (Meinshausen et al., 2020). In addition to the above, the ocean temperature and salinity were perturbed in the coupled atmosphere-ocean simulations. For the adjusted 3D variables in both the atmosphere and coupled models such as air and ocean temperatures, the climate change perturbations were added at all vertical levels in the atmosphere and ocean. Both models adjusted to the added perturbations within a few hours, thus, we used the first six simulated hours of the TC lifetime as spin-up and excluded these from all analyses. Supplementary Fig. 1 shows the E3SM September climatology of 2-m temperature and SST for the historical and future (i.e., SSP5-8.5) periods, as well as the estimated difference between the two periods used to perturb the initial and boundary conditions for the PGW simulations. Due to limited computing resources, we only used climate change perturbations from one global model for the atmosphere-only and coupled simulations. Thus, we did not account for uncertainty due to the range of climate sensitivities among different global models. Our results here, therefore, apply to the climate sensitivity of the E3SM.

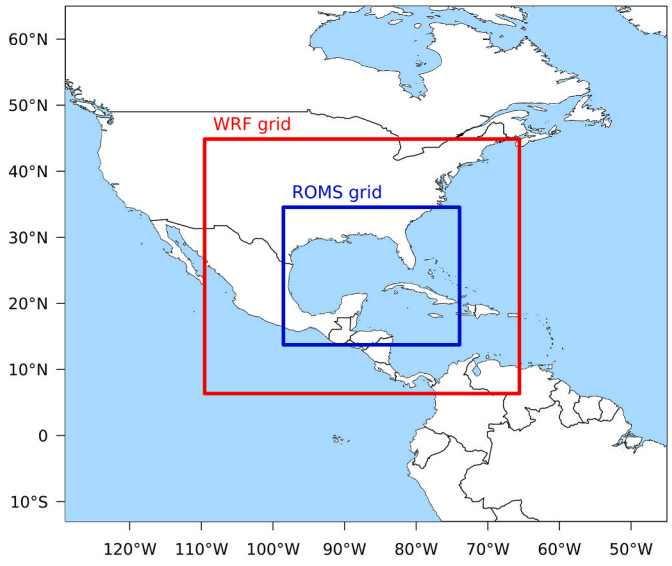

Fig. 1. Model simulation domains for atmosphere (WRF) and ocean (ROMS) models used to simulate Gulf Coast tropical cyclones including Hurricanes Ida, Michael, and Nate.

2.4. Detection of simulated TC tracks

Simulated TCs were identified using the location of the minimum sea level pressure (SLP). The simulated TCs in both the historical and PGW simulations were tracked for the same time period (Supplementary Table 1). To evaluate the response of TCs to anthropogenic changes, it was necessary to verify that hindcasted TCs could realistically represent the observed TC evolution, especially its track (Wehner et al., 2019). For this, we used observations from HURDAT2 (Landsea and Franklin, 2013) as archived in the International Best Track Archive for Climate Stewardship (IBTrACS) version 4 (Knapp et al., 2010) to evaluate the historical TC simulations. TC tracks simulated with both the atmosphere-only and coupled models were compared to observations (Fig. 2).

Hurricane Arthur's track was poorly hindcasted and was thus omitted from the remaining analyses. Ensemble mean historical tracks for the remaining TCs reasonably represented their corresponding observed tracks with only slight deviations for Irma and Michael (Fig. 2). Nate's historical track was similar to Michael, although Nate was moving at a much faster forward speed (Supplementary Fig. 2). Simulated historical TC tracks for both atmosphere-only and coupled simulations were nearly identical in all cases. This is not surprising as many previous studies have shown that TC tracks have little sensitivity to atmosphere-ocean coupling (e.g., Wu et al. (2005)). This is also true for individual ensemble members for all TCs (Supplementary Figs. 3a–d). We further evaluated the intensity of hindcasted TCs and found that the intensity of simulated TCs was underestimated (Supplementary Fig. 3e-p), likely due to the horizontal resolution. This is not surprising as TC intensity is usually underestimated for scales exceeding a few kilometers (Davis, 2018). This may introduce some uncertainty, which was not accounted for in this study due to limited supercomputing resources. Nevertheless, this uncertainty is unlikely to influence the sign of the projected TC statistics as shown by Patricola and Wehner (2018). Moreover, the temporal and spatial evolution of the observed TC intensity is hindcasted with reasonable fidelity. More importantly, the impact of TC-ocean interaction on the intensity of the hindcasted TCs can be clearly seen (Supplementary Fig. 3i-p), as many previous studies have shown that air-sea coupling significantly reduces intensity of TCs (e.g., Bender and Ginis, 2000; Emanuel, 1999; Wu et al., 2005).

3. Results

3.1. Influence of ocean coupling on the anthropogenic TC rainfall response

We investigated the response of TC rainfall to anthropogenic climate change and the influence of ocean coupling on the response by focusing on a reference region spanning a 500 km radius around the TC center throughout the TC lifetime (referred to as the composite). As in previous

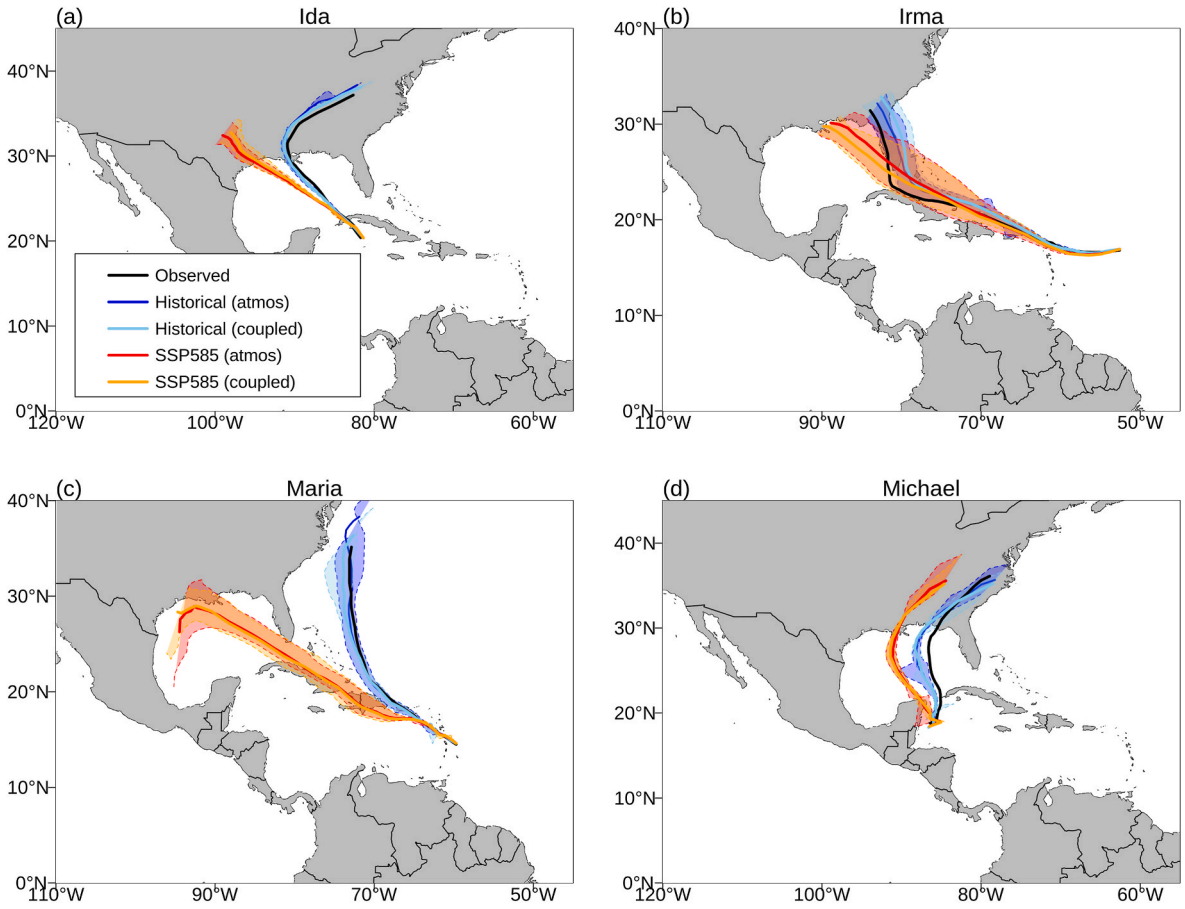

Fig. 2. Comparison of observed (black) and ensemble mean historical TC tracks simulated with atmosphere-only (solid blue) and coupled (solid light blue) models for Hurricanes (a) Ida, (b) Irma, (c) Maria, and (d) Michael. The solid red and orange lines show the ensemble mean response of historical TC tracks to anthropogenic climate change in the atmosphere-only and coupled simulations respectively. The shadings represent the ensemble spread of the simulated TC tracks. The dashed lines bounding the shadings represent the maximum and minimum range of longitudes and latitudes of the simulated TC tracks across all ensembles. The period for which each TC is tracked is shown in Supplementary Table 1.

studies (e.g., Knutson et al., 2010, 2020), TC rainfall increases in the future with or without ocean coupling (Fig. 3 and Supplementary Fig. 4). In addition to rainfall increases, the size of each of the TCs that we investigated increases in the future as shown by the larger spatial extent of the 18 ms^{-1} wind speed (Fig. 3 red contours). This increase was higher for TCs that were relatively small in the historical period (Supplementary Table 2). The largest rainfall increases in both atmosphere-only and coupled simulations occurred in the inner areas of the TCs, where rainfall was heaviest in the historical period. Rainfall increases near the storm center are consistent with Knutson et al. (2010) and Patricola & Wehner (2018).

It must be noted that the tracks of the simulated TCs robustly respond to the E3SM climate change perturbations, with westward displacements relative to the historical period that are considerable for some TCs such as Maria (Fig. 2). The westward shifts could be due to changes in deep-layer environmental flow, which have been identified as being responsible for similar westward shifts in Atlantic TC tracks (Kelly et al., 2018). However, we only model several storms in this study and consequently caution that these results may not be applicable to the full Atlantic basin. The displacements of TC tracks therefore imply that rainfall increases in the warmer climate may not only be attributed to the thermodynamic effects of climate change but also the TC's local interaction with its new environment. However, we expect the latter's effect to be minimal, especially given that the large future rainfall increase for Hurricane Irma—whose historical and future tracks are similar for most of its lifetime (Fig. 2b)—are reproduced in the other TCs (Fig. 3). Hurricane Irma's rainfall for only the parts of the historical and future tracks with minimal deviations is shown in Supplementary Fig. 5.

As shown by Trenberth et al. (2007), the moisture budget of TCs is dominated by the inflow of moisture in the lowest 1 km of the TC, driven by the surrounding winds. We therefore compared the concurrent mean water vapor mixing ratio integrated from the surface to 800 hPa within a radius of 1000 km from the TC center (Fig. 4). Here, we see that both historical and PGW simulations have similar spatial distributions of water vapor. However, the amount of water vapor in the PGW simulations is much larger than the historical simulations whether in the atmosphere-only or coupled model. This largely explains the increased rainfall in the future simulations for all TCs. Based on the Clausius-Clapeyron relation, the higher water vapor in the PGW simulations is due to increased water-holding capacity of the atmosphere following the increased temperature in the future climate. In both historical and future simulations, most of the water vapor comes from outside the precipitation area of the TC, defined here as the 500 km radius around the TC (pink circle). In the lower atmosphere, the environmental winds, and the winds in the outer core of the TCs (arrows) appear to draw this water vapor into the storm core. This is then lifted upward, with the largest upward motions found within the core of the TC as shown by the higher vertical velocity (white contours). This mechanism could partly explain why the largest rainfall change between the historical and future climates occurs in the inner areas of the TCs.

A secondary mechanism that could explain the future rainfall increase and especially, why the largest increase occurs in the inner areas is the ocean-surface heat fluxes. These fluxes strongly influence the intensity of the TCs. Fig. 5 shows the mean ocean-surface enthalpy flux

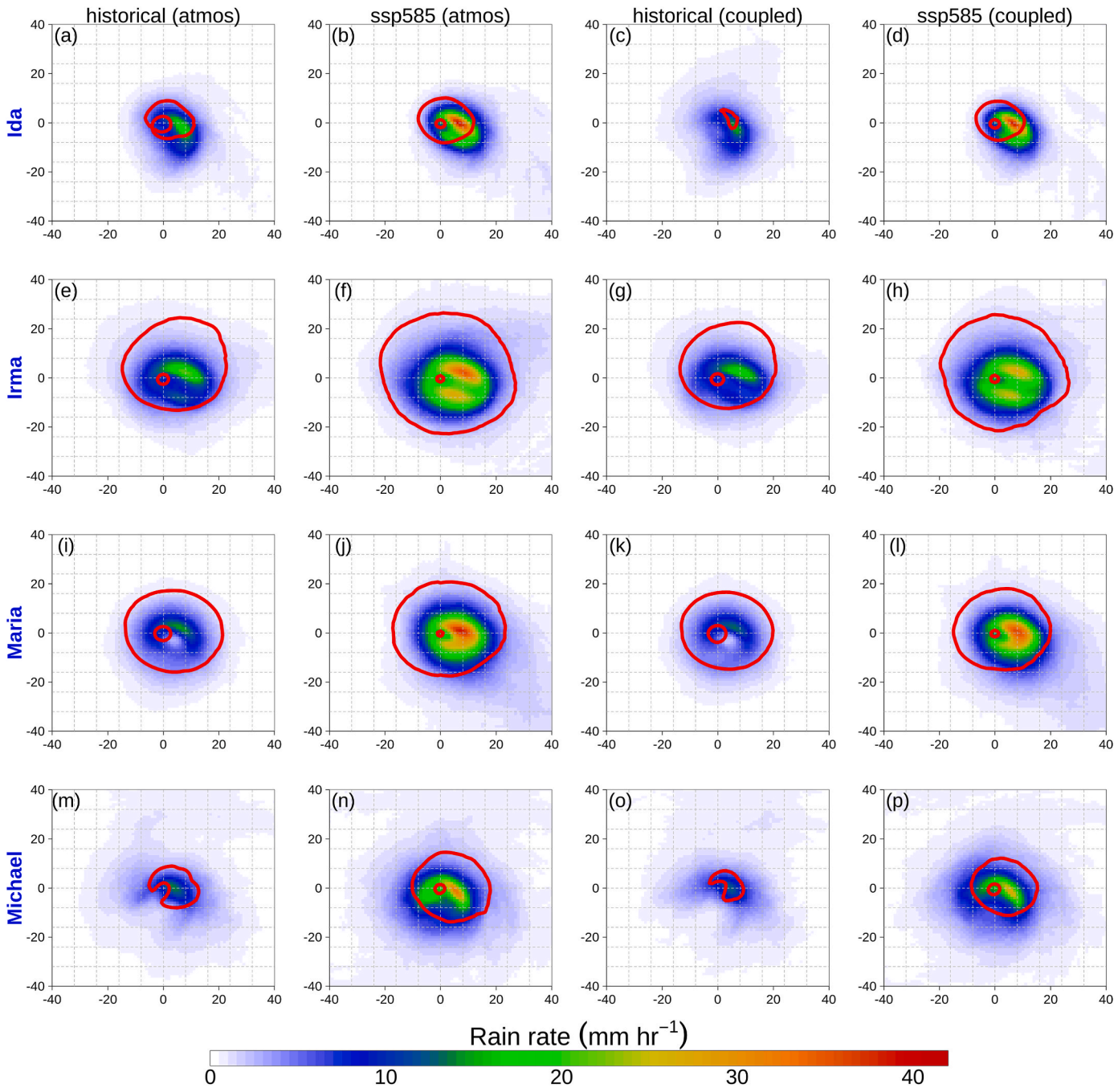

Fig. 3. Simulated ensemble mean TC rainfall rate (mm hr^{-1}) composited within a 500 km radius around the tropical cyclone center throughout its lifetime for atmosphere-only: (a, e, f, m) historical and (b, f, j, n) SSP5-8.5, and coupled: (c, g, k, o) historical and (d, h, l, p) SSP5-8.5 simulations for Hurricanes (a–d) Ida, (e–h) Irma, (i–l) Maria, and (m–p) Michael. The red contours represent the ensemble mean 18 ms^{-1} wind speed location. The x and y axes indicate the number of grid cells from the TC center.

within a radius of 500 km (comparable to the pink circle in Fig. 4). As expected, the ocean-surface enthalpy flux is higher in the PGW simulations. The implication for this is locally enhanced kinetic energy (Rotunno and Emanuel, 1987), which in turn increases TC intensity and the secondary circulation associated with the TC (Emanuel, 1997). The stronger TC winds help to import water vapor into the storm. For all TCs in this study, the strongest enthalpy flux is found in the inner TC core, suggesting a strong influence from the underlying ocean and the high wind speed at the inner core region. This together with the water vapor inflow from beyond the precipitation area (pink circle in Fig. 4) could explain why the local maxima of water vapor appears in the TC inner core. In addition, the enthalpy flux is lower in the coupled simulations than the atmosphere-only simulations whether in the historical or future climate for all TCs. This is an indication that the water vapor inflow due to TC winds and evaporation may be weaker in the coupled model than in the atmosphere-only model, which could explain the lower rainfall rate in the inner TC core areas in the coupled model.

Statistical significance of TC rainfall increases was then evaluated using a Student's t-test. We determined the average 500 km radius rainfall around the TC center for all ensemble members, following prior research (e.g., Matyas 2013). For all TCs, the projected increase of TC rainfall was statistically significant at the 5 % level for both uncoupled and coupled simulations (Table 1). The rainfall increase magnitude was lower in the coupled simulations, however. This was also true whether

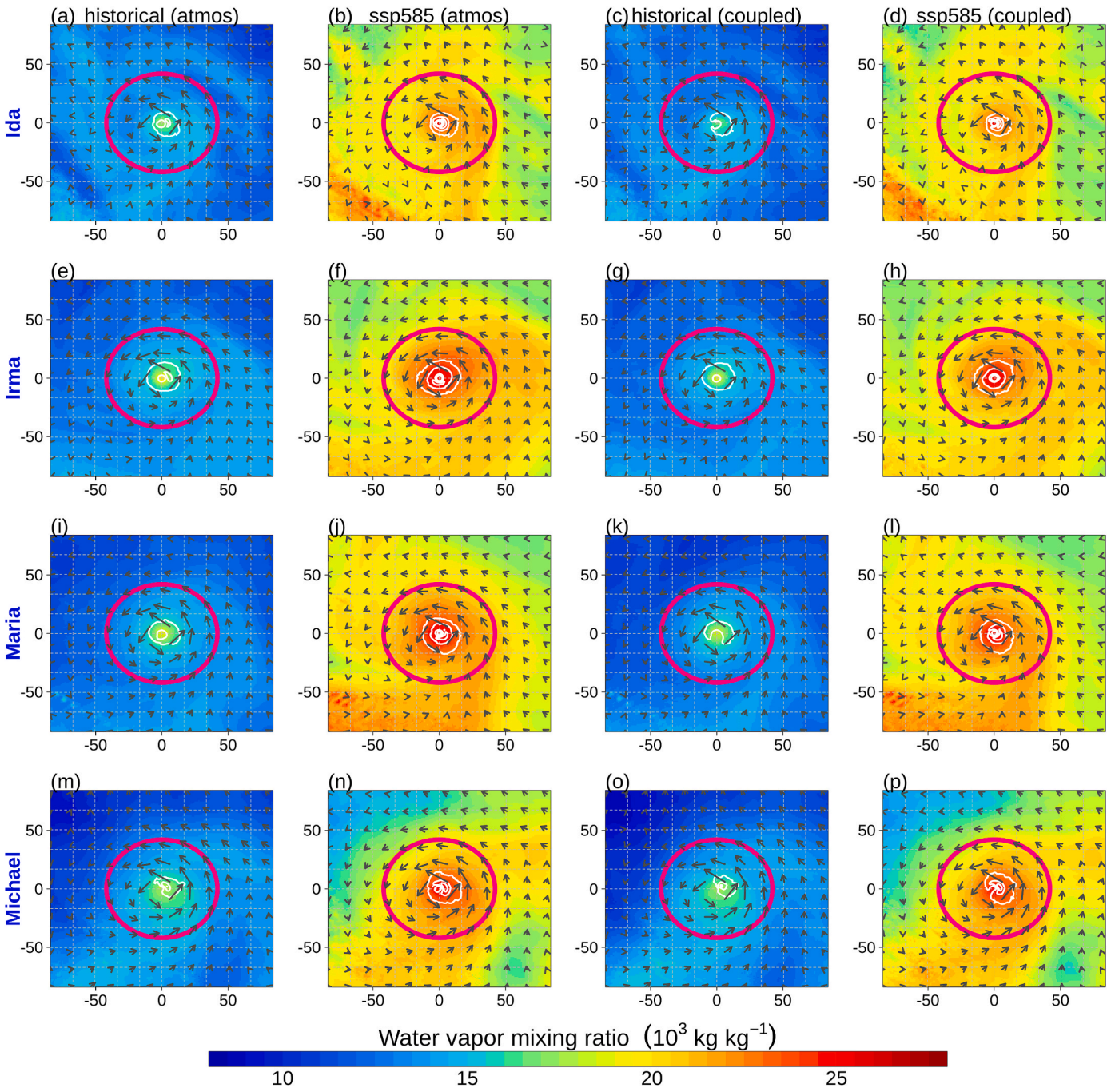

Fig. 4. Ensemble mean simulated water vapor mixing ratio (10^3 kg kg^{-1}) composited within a 1000 km radius around the tropical cyclone center throughout its lifetime for atmosphere-only: (a, e, f, m) historical and (b, f, j, n) SSP5-8.5, and coupled: (c, g, k, o) historical and (d, h, l, p) SSP5-8.5 simulations for Hurricanes (a–d) Ida, (e–h) Irma, (i–l) Maria, and (m–p) Michael. The arrows are the environmental wind direction from the surface to 800 hPa. The pink circle represents a 500 km radius region around the TC center. The white contours represent the ensemble mean positive vertical velocity (cm s^{-1}) averaged over all vertical levels from the surface throughout the TC lifetime; only three contour levels (0.1, 0.3, and 0.5 cm s^{-1}) are shown with the highest values in the innermost areas of the TCs. The x and y axes indicate the number of grid cells from the TC center.

TC rainfall was computed over only the ocean (Supplementary Fig. 6) or land (Supplementary Fig. 7). Although the increase in TC rainfall agrees with the findings of previous studies that were also based on PGW simulations (Patricola and Wehner 2018), the magnitudes are substantially larger in our study. For instance, Hurricane Irma's rainfall average is projected to increase by 86 % and 83 % relative to the historical period for uncoupled and coupled simulations respectively, compared to a 27 % increase in the uncoupled simulations of Patricola & Wehner (2018) based on the RCP8.5 emission scenario. This is likely due to the differences in the global climate models used to provide climate change perturbations in the two studies. In the study of Patricola & Wehner (2018), the response of TC activity to high-end anthropogenic climate change may have been conservative. This is because the driving climate change perturbations used in the study were estimated from the Community Climate System Model (CCSM4) (Gent et al., 2011), whose sensitivity is among the lower end of CMIP5 global models (Andrews et al., 2012; Vial et al., 2013). Therefore, the driving GCM could influence the projected TC response.

The large future rainfall increases found in this study for most TCs cannot be explained by the Clausius-Clapeyron scaling (~7 % °C^{-1})

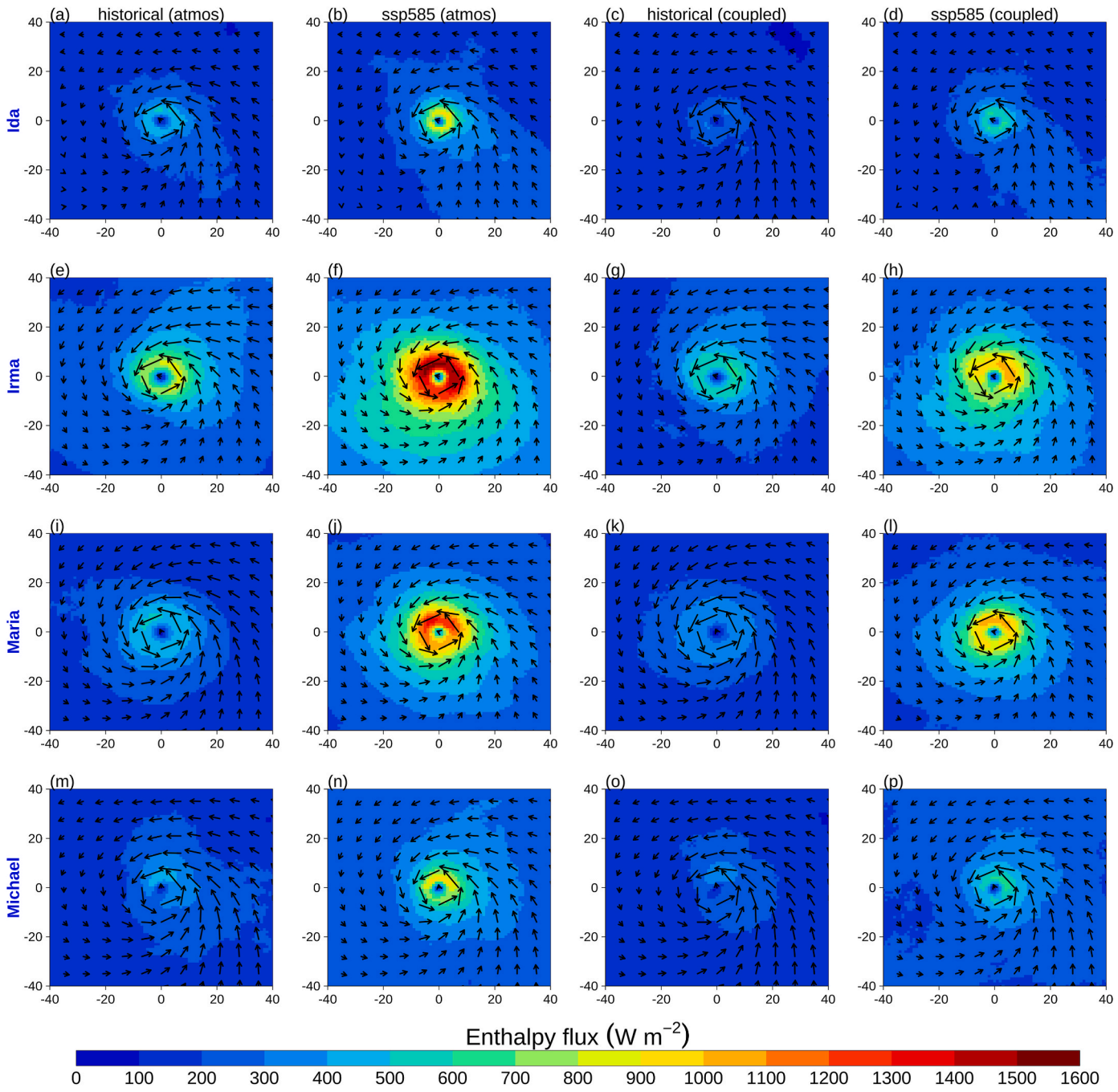

Fig. 5. Ensemble mean ocean-surface enthalpy flux (W m^{-2}) composites within a 500 km radius around the TC center throughout its lifetime for atmosphere-only: (a, e, f, m) historical and (b, f, j, n) SSP5-8.5, and coupled: (c, g, k, o) historical and (d, h, l, p) SSP5-8.5 simulations for Hurricanes (a–d) Ida, (e–h) Irma, (i–l) Maria, and (m–p) Michael. The arrows represent the average 10-m wind direction. The x and y axes indicate the number of grid cells from the TC center.

alone. For instance, our finding for the rainfall increase of Hurricane Irma requires the temperature increase to be ~12 °C for the Clausius-Clapeyron scaling to hold. This is however not the case, as both the estimated 2-m temperature and SST increases based on the E3SM is < 10 °C throughout the model domain (Supplementary Fig. 1). Previous studies have shown that this "super Clausius-Clapeyron" scaling is likely due to other factors such as TC intensity increases (Hallam et al., 2023; Liu et al., 2019). By excluding the impact of storm intensity, Liu et al. (2019) showed that the rainfall rate increases matched better with the Clausius-Clapeyron rate than when the influence of storm intensity was not excluded. Their finding suggests that the "super Clausius-Clapeyron scaling" of rainfall rates with temperature increase as shown in this study and others (e.g., Reed et al. (2020)), is due to anthropogenic warming-induced increases in TC intensity.

Since TC size increases from the historical to the future climate (red contours, Fig. 3), regions affected by the heaviest TC rainfall are likely to increase. Therefore, we also estimated average TC rain over the regions of heaviest rainfall, defined as all grid points exceeding 2 and 1 mm h^{-1}, respectively. We found that extreme TC rainfall increases with or without ocean coupling but the magnitude varies substantially depending on whether the simulations are coupled or not (Table 1). Thus, the influence of ocean coupling on the magnitude of extreme TC rainfall change may depend on individual TC characteristics.

Table 1
Simulated ensemble mean difference in rainfall rate between the SSP5-8.5 and the historical period expressed as a percentage of the historical average over a 500 km radius region around the TC center and a region of concentrated rainfall around the TC with rain rates > 2 and 1 mm h^{-1} for atmosphere-only and coupled simulations. All changes are significant at the 5 % level.

TC	(SSP5-8.5 – historical)/historical					
	500 km radius		> 2 mm h^{-1}		> 1 mm h^{-1}	
	atmos	coupled	atmos	coupled	atmos	coupled
Ida	34	14	55	80	39	97
Irma	86	83	37	44	33	38
Maria	143	125	69	80	46	45
Michael	99	90	52	39	61	57
Nate	63	52	71	64	92	81

Table 2
Simulated ensemble mean difference in 10-m maximum wind speed and minimum sea level pressure between the SSP5-8.5 and the historical period expressed as a percentage of the historical average for atmosphere-only and coupled simulations. All changes are significant at the 5 % level.

Intensity metric	TC	(SSP5-8.5 – historical)/historical	
		atmos	coupled
Maximum wind speed	Ida	32	31
	Irma	35	36
	Maria	38	46
	Michael	49	42
	Nate	33	30
Minimum sea level pressure	Ida	−3.5	−3.1
	Irma	−5.4	−5
	Maria	−5	−4.9
	Michael	−5.5	−4.4
	Nate	−1.6	−1.2

3.2. Influence of ocean coupling on anthropogenic TC intensity response

We then investigated the response of TC intensity to anthropogenic climate change by evaluating differences in ensemble mean maximum 10-m wind speed and minimum SLP during the TC lifetime between the historical and future simulations. In our simulations, TC intensities are generally lower when the atmosphere and ocean are coupled, whether in the historical or future climate (Fig. 6). This result is similar to findings from some previous studies with global models (e.g., Li and Sriver (2018; 2019)). The difference could be explained by lower air-sea enthalpy fluxes found in the coupled simulations (Fig. 5). However, the intensity of all TCs in both atmosphere-only and coupled simulations increases in the warmer climate (Fig. 6 and Table 2). Therefore, this is robust evidence that ocean coupling does not influence the sign of the anthropogenic TC intensity response in the five TCs that were studied. The increase of TC intensity is statistically significant at the 5 % level for all TCs.

Our results further showed that the magnitude of TC increase from the historical to future climates in the atmosphere-only (32–49 % for wind speed and −1.6 to −5.5 % for SLP) was comparable to the coupled (30–46 % for wind speed and −1.2 to −5 % for SLP) simulations (Table 2). Thus, at least for the TCs considered in this study, ocean coupling appears to have a modest influence on the magnitude of the anthropogenic TC intensity response. Despite this, we found that future intensity increases in the atmosphere-only simulations were always higher, albeit slightly, than the coupled simulations for all of the TCs considered when using SLP as a metric for TC intensity. This is however not always true when considering the maximum sustained wind speed, as in some cases the coupled simulations project higher intensity increases. This result may not necessarily be reproduced for other TCs and thus cannot be generalizable. A larger number of TC cases may however help to better understand this in future studies.

3.3. Enhanced tropical cyclone induced cooling in coupled simulations

Cold SST anomalies due to a TC passage have profound impacts on TC intensification (Mei et al., 2013; Mei et al., 2015b) and the post-TC atmospheric environment (Ma et al., 2020). Comparing the pre- and post-TC SST difference between the atmosphere-only and coupled simulations for the SSP5-8.5 future simulations (Fig. 7), we find that, as expected, TC-induced cooling is larger in the latter in which the ocean responds to the TC than in the former, with prescribed SST. This is also

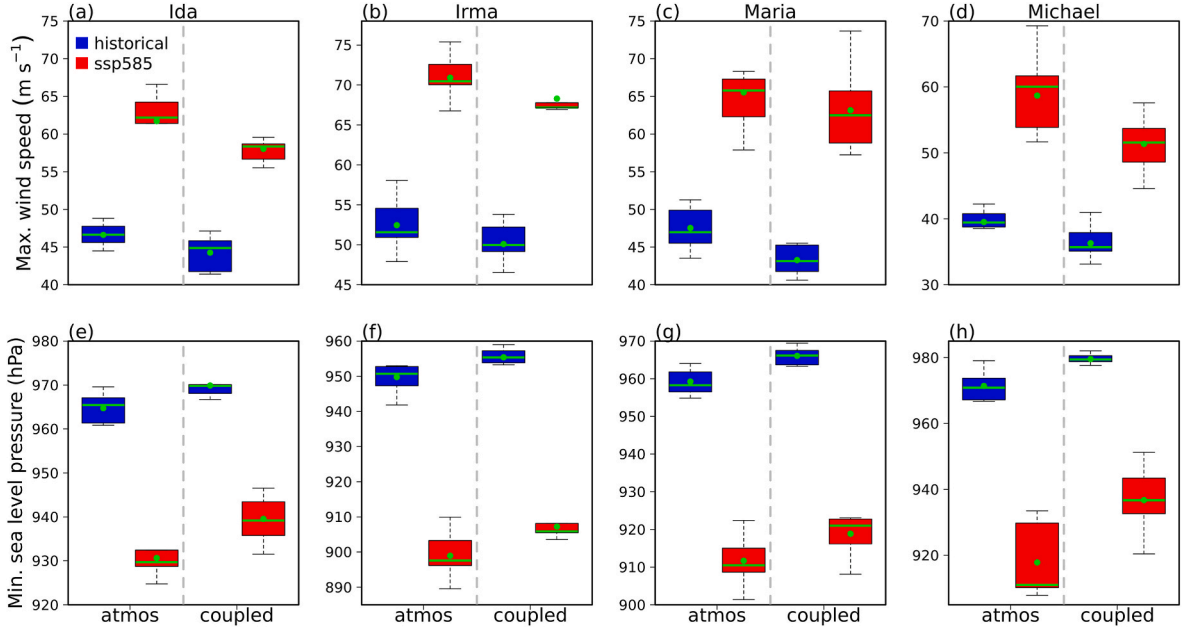

Fig. 6. (a–d) Boxplots of simulated maximum TC lifetime intensity based on 10-m wind speed (m s^{-1}) from the 10-member ensemble of atmosphere-only and coupled simulations of Hurricanes (a) Ida, (b) Irma, (c) Maria, and (d) Michael for the historical (blue) and SSP5-8.5 (red) periods. (e–h) as in a-d but for minimum sea level pressure (hPa). The green dot and line represent the ensemble mean and median maximum intensities, respectively. The red and blue boxes denote the interquartile range, and whiskers denote the minimum and maximum.

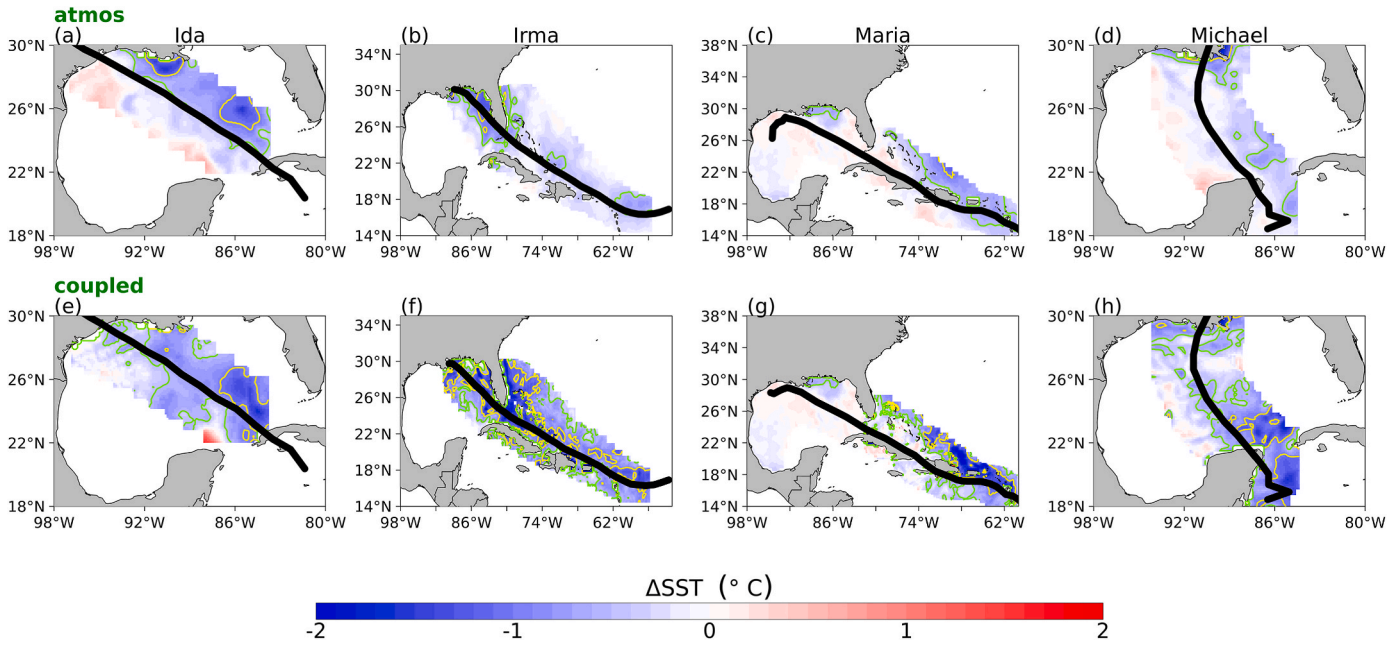

Fig. 7. (a–d) Time slices of ensemble mean SST change defined as $\Delta SST = SST_{+2\_days} - SST_{-2\_days}$ at each TC location for atmosphere-only simulations of Hurricanes (a) Ida, (b) Irma, (c) Maria, and (d) Michael in the SSP5-8.5 scenario. (e–h) as in a-d but for coupled simulations. Areas of the ocean which are not within a 200 km radius of the TC center are blanked for clarity. Cooling levels of −1 and −0.5 °C are shown by yellow and green contours, respectively. The black lines represent the simulated TC track.

true for the historical simulations (Supplementary Fig. 8). The relatively weaker SST cooling seen in the atmosphere-only simulations could be attributed to the cold wakes that already existed in the reanalysis data used to prescribe the SST. The enhanced cold wake in the coupled simulations could explain the lower air-sea enthalpy flux (Fig. 5), which could have a profound impact on the atmosphere, subsequently reducing TC intensity and future development (Karnauskas et al., 2021). This could further explain why most coupled GCMs project lower TC frequency in the future than their atmosphere-only counterparts (Roberts et al., 2020).

TC-induced cooling also suppresses both clouds and rainfall in the wake regions (Ma et al., 2020), potentially impacting projected TC rainfall statistics. The definition of TC rainfall composites means that composited rainfall at a given time step could include a substantial portion of the previous time step's composite, which would now be in the cold wake region. Enhanced cold wakes in the coupled simulations could explain the lower magnitude of projected rainfall increases when considering a 500 km radius around the TC center (Table 1). The magnitude of future TC rainfall increase varies considerably depending on whether the simulations are coupled or not when considering the

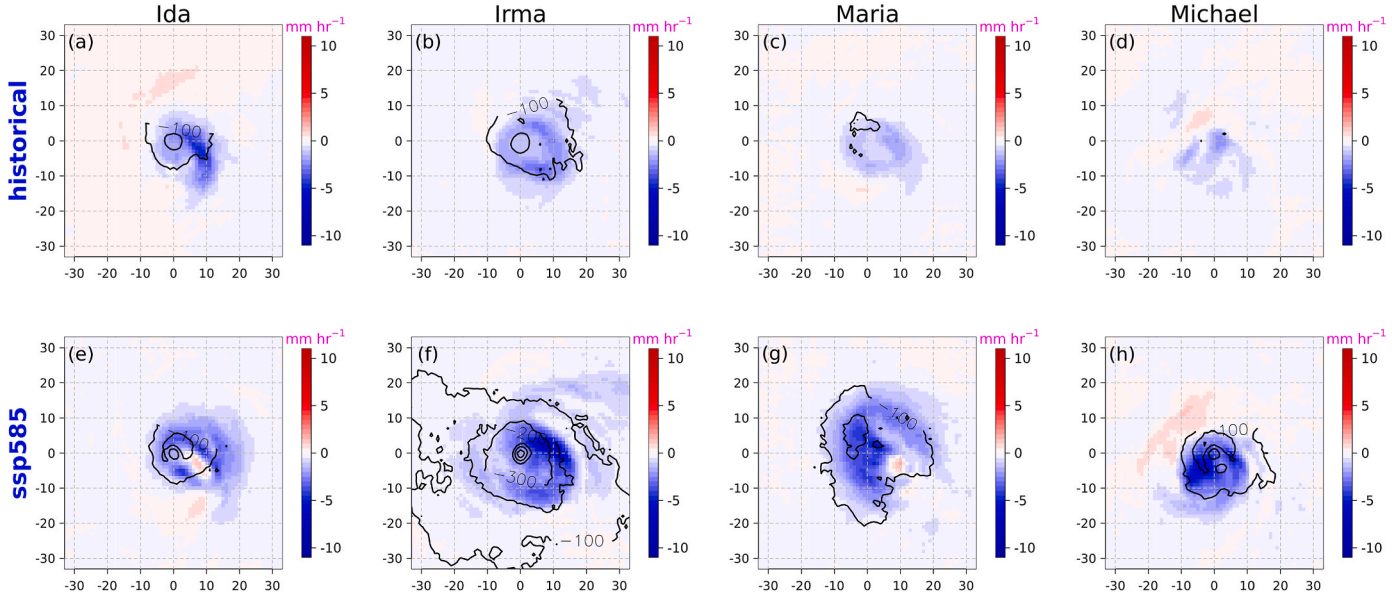

Fig. 8. Ensemble mean difference in simulated TC rainfall rate (mm hr^{-1}) between coupled and atmosphere-only simulations for the (a–d) historical and (e–h) SSP5-8.5 periods for Hurricanes (a, e) Ida, (b, f) Irma, (c, g) Maria, and (d, h) Michael. Differences are determined from composites of rainfall rate composited relative to the TC center throughout its lifetime. The contours represent ensemble mean differences in surface latent heat fluxes (Wm^{-2}). The x and y axes indicate the number of grid cells from the TC center.

areas of heaviest rainfall near the storm center. Therefore, subject to different rainfall measures and definition, coupled simulations may not always lead to a lower magnitude of projected future TC rainfall increases than atmosphere-only simulations.

3.4. Sensitivity of ocean coupling: Historical vs. PGW simulations

We further investigated whether differences in TC statistics between the atmosphere-only and coupled simulations in the historical period could be modified in the future climate. This would allow us to determine the sensitivity of atmosphere-ocean coupling to warmer temperatures. For TC rainfall, our results have shown that atmosphere-only simulations generally lead to higher values than coupled simulations, whether in the historical or future period (Fig. 3). However, for all of the TCs considered here, the magnitude of the rainfall difference between atmosphere-only and coupled simulations is much larger in the future climate, reaching up to five times for some TCs (Fig. 8 and Table 3). This is an indication that the uncertainty of TC rainfall estimates in historical simulations due to the lack of atmosphere-ocean coupling may be magnified further in warmer conditions. This could be explained by changes in the upper ocean thermal structure in addition to individual TC characteristics in the future climate. For example, in the case of Irma, the increase in the depth of the 26 °C isotherm (Fig. 9) increases the ocean heat content (Lin et al., 2008). A similar response is seen for all the other TCs considered in this study (not shown). This increase in ocean heat content explains the future rainfall increase due to increased evaporation and moisture content in the TC environment (Trenberth et al., 2018). However, the intensity of the TC-induced cooling is much higher in the entire warm layer in the future than in the historical climate. This could be due to increased wind speeds, which enhances vertical mixing and upwelling of cooler ocean water, consequently reducing ocean-surface latent heat fluxes (Fig. 8 contours). We note however that this process may depend on individual TC characteristics and location.

On the other hand, the magnitude of intensity difference between atmosphere-only and coupled simulations tends to depend on the metric used to characterize TC intensity. Like rainfall, the magnitude of the changes is always larger in the future climate when using minimum SLP (Table 3). The magnitude of the difference reaches more than a factor of two for some of the TCs. On the contrary, the magnitude of the intensity difference is not always larger in the future climate when using the maximum 10-m wind speed. For example, the magnitude difference between the atmosphere-only and coupled simulations for Hurricanes Irma and Maria is 4.6 % and 8.8 % respectively in the historical period. In the future period, the magnitude difference is 3.7 % and 3.5 % respectively, although both were not statistically significant. A better understanding of the pattern of these differences could be established by using a higher number of TC cases in future studies.

Table 3
Ensemble mean percent difference in simulated TC 10-m maximum wind speed, minimum sea level pressure, and rain rate between coupled and atmosphere-only simulations for the historical and SSP5-8.5 periods. Changes denoted by * are significant at the 5 % level.

	TC	(coupled – atmos)/atmos	
		historical	SSP5-8.5
Maximum wind speed	Ida	−4.9*	−6*
	Irma	−4.6	−3.7
	Maria	−8.8*	−3.5
	Michael	−8.1*	−12.4*
	Nate	−8.9	−10.8
Minimum sea level pressure	Ida	0.5*	1*
	Irma	0.6*	0.9*
	Maria	0.7*	0.8*
	Michael	0.8*	2.1*
	Nate	0.6	1.1
Rain rate	Ida	−3.6*	−18*
	Irma	−14.8*	−16*
	Maria	−8.6*	−15.3*
	Michael	−7.6*	−11.9*
	Nate	−6.7	−12.8

4. Summary and conclusion

This study has shown the importance of accounting for atmosphere-ocean interaction in numerical model projections of future TC activity. The response of TC activity to anthropogenic climate change was investigated using both atmosphere-only and coupled simulations of several recent impactful TC events. We first simulated the TC events in the historical conditions in which they occurred and then simulated the same events in a high-emission warm scenario at the end of the 21st century based on projections from the E3SM. Our results showed that the rainfall and intensity of several recent hurricane events would increase if they were to occur in much warmer conditions, whether simulations are made with an atmosphere-only or coupled model. Consequently, this allows us to have confidence in projections based on atmosphere-only models, as most project increasing intensity and rainfall, albeit with varying magnitudes (Knutson et al., 2013; Villarini et al., 2014; Wright et al., 2015).

However, by accounting for atmosphere-ocean interactions, the magnitude of the future increase of TC rainfall and intensity is influenced, albeit slightly in the latter. Over a 500 km radius around the simulated TCs, our coupled simulations led to a 3–47 % less projected rainfall increase than the atmosphere-only simulations. The differences were found to be driven by enhanced TC-induced cooling in the coupled simulations for all of the simulated TCs. When considering the regions of heaviest rainfall around the TC, however, the influence of coupling on the increase in magnitude varied considerably. Using a 2 mm h^{-1} threshold, for instance, the magnitude of TC rainfall increase could be up to 25 % less or 13 % more than the atmosphere-only simulations. This indicates that the local-scale influence of TC-ocean coupling and heterogeneity depends on individual storm characteristics. The influence of atmosphere-ocean interactions on the magnitude of future intensity increase was not as large as for rainfall, with a range of 32–49 % and 30–46 % in 10-m wind speed increases for the atmosphere-only and coupled simulations, respectively.

Comparing the differences in TC statistics between atmosphere-only and coupled simulations of the historical period to the future period revealed a possible sensitivity of TC-ocean interaction to climate change. We found that the magnitude of the difference between simulated atmosphere-only and coupled TC rainfall was much larger in the future period (up to a factor of five for some TCs) than in the historical period. This suggests that the influence of atmosphere-ocean interactions on simulated hurricane rainfall statistics may be sensitive to warming for the simulated hurricane events. Additionally, although TC rainfall tends to be greater in atmosphere-only simulations compared to coupled simulations, this response is substantially more pronounced in the future climate compared to the historical, indicating that using prescribed SSTs may introduce much greater errors in simulations of the future climate compared to the historical. For TC intensity, the differences in the magnitude were small and dependent on the metric used to characterize intensity.

A limitation of our study was the use of one GCM (i.e., E3SM) to provide the driving climate change perturbations. Therefore, our projections correspond to a given level of warming, which could happen later or earlier in time than it does in the E3SM. It also means that the TC response shown in this study applied to the climate sensitivity of E3SM only and did not account for uncertainty due to the range of climate sensitivities among different models. Thus, our results may not necessarily be generalizable. Different climate sensitivities due to the underlying global model could lead to substantial differences in the TC response. Individual GCM biases may also impact the TC response to climate change. Therefore, further PGW simulations with climate

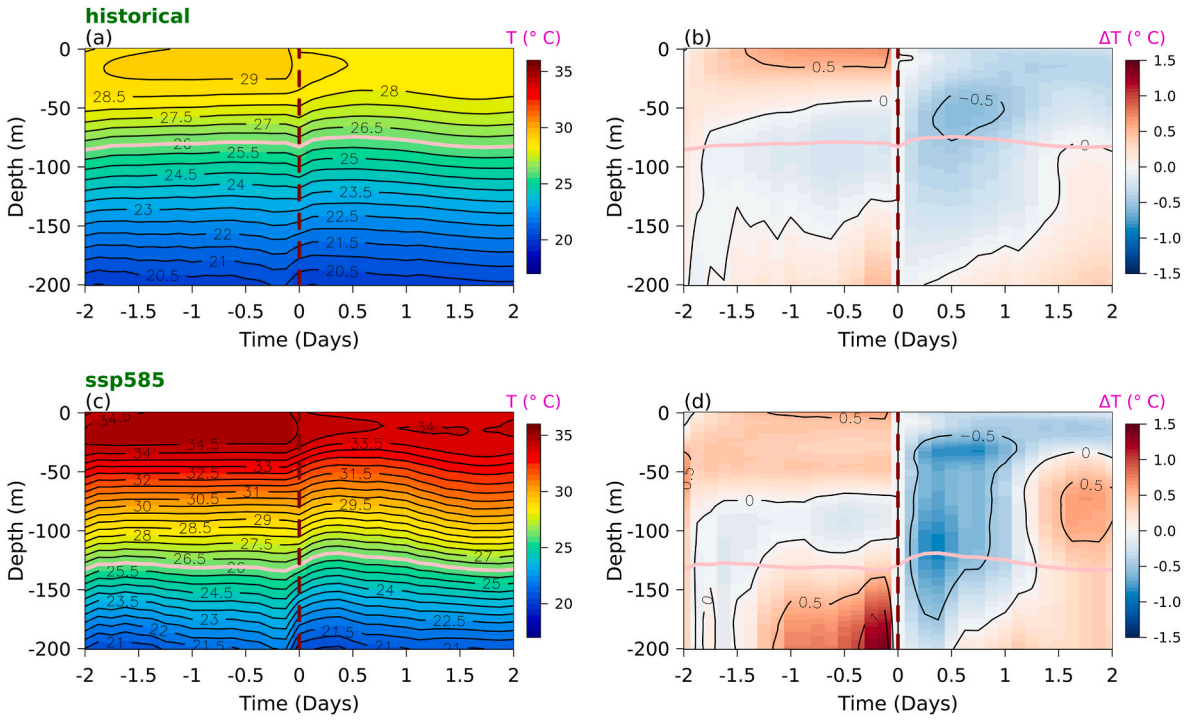

Fig. 9. (a–b) Vertical (a) temperature and (b) temperature anomalies before and after TC passage averaged over all locations over the ocean for the historical simulation of Hurricane Irma. (c–d) as in (a–b) but for the SSP585 simulation. The black contours also represent different levels of the temperature or temperature anomaly. The pink contour represents the 26 °C isotherm. The dashed brown line represents the mean vertical profile of the temperature when the TC is present (i.e., Time = 0). The anomalies are calculated by subtracting the temperature at Time = 0 from each time step.

change perturbations from multiple GCMs are planned to investigate this uncertainty.

Code availability

The code for the COAWST system, which includes the codes for both the ROMS and WRF models, is available at https://github.com/jcwarner-usgs/COAWST. All analysis codes are available from the corresponding author on request.

CRediT authorship contribution statement

Derrick K. Danso: Conceptualization, Formal analysis, Investigation, Methodology, Software, Visualization, Writing – original draft. **Christina M. Patricola:** Conceptualization, Funding acquisition, Methodology, Project administration, Resources, Supervision, Writing – review & editing. **Jaison Kurian:** Methodology, Writing – review & editing. **Ping Chang:** Writing – review & editing. **Philip Klotzbach:** Writing – review & editing. **I.-I. Lin:** Writing – review & editing.

Declaration of competing interest

The authors declare that they have no known competing financial interests or personal relationships that could have appeared to influence the work reported in this paper.

Data availability

Data will be made available on request.

Acknowledgements

This material is based upon work supported by the U.S. Department of Energy, Office of Science, Office of Biological and Environmental Research (BER), Earth and Environmental Systems Modeling (EESM) Program, under Early Career Research Program Award Number DE-SC0021109 and under Award Number DE-AC02-05CH11231. This research used resources of the National Energy Research Scientific Computing Center (NERSC), a U.S. Department of Energy Office of Science User Facility located at Lawrence Berkeley National Laboratory, operated under Contract No. DE-AC02-05CH11231. We wish to also thank the developers of the COAWST modeling platform. P. Klotzbach acknowledges funding from the G. Unger Vetlesen Foundation. We thank one anonymous reviewer for their constructive feedback that has helped improve the manuscript.

Appendix A. Supplementary data

Supplementary data to this article can be found online at https://doi.org/10.1016/j.wace.2024.100649.

References

Andrews, T., Gregory, J.M., Webb, M.J., Taylor, K.E., 2012. Forcing, feedbacks and climate sensitivity in CMIP5 coupled atmosphere-ocean climate models. Geophys. Res. Lett. 39 (9) https://doi.org/10.1029/2012GL051607 n/a-n/a.

Balaguru, K., Chang, P., Saravanan, R., Leung, L.R., Xu, Z., Li, M., Hsieh, J.-S., 2012. Ocean barrier layers' effect on tropical cyclone intensification. Proc. Natl. Acad. Sci. USA 109 (36), 14343–14347. https://doi.org/10.1073/pnas.1201364109.

Bender, M.A., Ginis, I., 2000. Real-case simulations of hurricane–ocean interaction using A high-resolution coupled model: effects on hurricane intensity. Mon. Weather Rev. 128 (4), 917–946. https://doi.org/10.1175/1520-0493(2000)128<0917:RCSOHO>2.0.CO;2.

Bhatia, K.T., Vecchi, G.A., Knutson, T.R., Murakami, H., Kossin, J., Dixon, K.W., Whitlock, C.E., 2019. Recent increases in tropical cyclone intensification rates. Nat. Commun. 10 (1), 635. https://doi.org/10.1038/s41467-019-08471-z.

Chassignet, E., Hurlburt, H., Metzger, E.J., Smedstad, O., Cummings, J., Halliwell, G., Bleck, R., Baraille, R., Wallcraft, A., Lozano, C., Tolman, H., Srinivasan, A., Hankin, S., Cornillon, P., Weisberg, R., Barth, A., He, R., Werner, F., Wilkin, J., 2009. US GODAE: global ocean prediction with the HYbrid coordinate Ocean Model (HYCOM). Oceanography 22 (2), 64–75. https://doi.org/10.5670/oceanog.2009.39.

Chen, S., Elsberry, R.L., Harr, P.A., 2017. Modeling interaction of a tropical cyclone with its cold wake. J. Atmos. Sci. 74 (12), 3981–4001. https://doi.org/10.1175/JAS-D-16-0246.1.
Davis, C.A., 2018. Resolving tropical cyclone intensity in models. Geophys. Res. Lett. 45 (4), 2082–2087. https://doi.org/10.1002/2017GL076966.
Dutheil, C., Lengaigne, M., Bador, M., Vialard, J., Lefèvre, J., Jourdain, N.C., Jullien, S., Peltier, A., Sultan, B., Menkès, C., 2020. Impact of projected sea surface temperature biases on tropical cyclones projections in the South Pacific. Sci. Rep. 10 (1), 4838. https://doi.org/10.1038/s41598-020-61570-6.
Emanuel, K., 2021. Response of global tropical cyclone activity to increasing CO2: results from downscaling CMIP6 models. J. Clim. 34 (1), 57–70. https://doi.org/10.1175/JCLI-D-20-0367.1.
Emanuel, K.A., 1997. Some aspects of hurricane inner-core dynamics and energetics. J. Atmos. Sci. 54 (8), 1014–1026. https://doi.org/10.1175/1520-0469(1997)054<1014:SAOHIC>2.0.CO;2.
Emanuel, K.A., 1999. Thermodynamic control of hurricane intensity. Nature 401 (6754), 665–669. https://doi.org/10.1038/44326.
Eyring, V., Bony, S., Meehl, G.A., Senior, C.A., Stevens, B., Stouffer, R.J., Taylor, K.E., 2016. Overview of the coupled model Intercomparison project phase 6 (CMIP6) experimental design and organization. Geosci. Model Dev. (GMD) 9 (5), 1937–1958. https://doi.org/10.5194/gmd-9-1937-2016.
Gent, P.R., Danabasoglu, G., Donner, L.J., Holland, M.M., Hunke, E.C., Jayne, S.R., Lawrence, D.M., Neale, R.B., Rasch, P.J., Vertenstein, M., Worley, P.H., Yang, Z.-L., Zhang, M., 2011. The community climate system model version 4. J. Clim. 24 (19), 4973–4991. https://doi.org/10.1175/2011JCLI4083.1.
Golaz, J., Caldwell, P.M., Van Roekel, L.P., Petersen, M.R., Tang, Q., Wolfe, J.D., Abeshu, G., Anantharaj, V., Asay-Davis, X.S., Bader, D.C., Baldwin, S.A., Bisht, G., Bogenschutz, P.A., Branstetter, M., Brunke, M.A., Brus, S.R., Burrows, S.M., Cameron-Smith, P.J., Donahue, A.S., et al., 2019. The DOE E3SM coupled model version 1: overview and evaluation at standard resolution. J. Adv. Model. Earth Syst. 11 (7), 2089–2129. https://doi.org/10.1029/2018MS001603.
Grinsted, A., Moore, J.C., Jevrejeva, S., 2013. Projected Atlantic hurricane surge threat from rising temperatures. Proc. Natl. Acad. Sci. USA 110 (14), 5369–5373. https://doi.org/10.1073/pnas.1209980110.
Guo, T., Sun, Y., Liu, L., Zhong, Z., 2020. The impact of storm-induced SST cooling on storm size and destructiveness: results from Atmosphere-Ocean coupled simulations. Journal of Meteorological Research 34 (5), 1068–1081. https://doi.org/10.1007/s13351-020-0001-2.
Haidvogel, D.B., Arango, H., Budgell, W.P., Cornuelle, B.D., Curchitser, E., Di Lorenzo, E., Fennel, K., Geyer, W.R., Hermann, A.J., Lanerolle, L., Levin, J., McWilliams, J.C., Miller, A.J., Moore, A.M., Powell, T.M., Shchepetkin, A.F., Sherwood, C.R., Signell, R.P., Warner, J.C., Wilkin, J., 2008. Ocean forecasting in terrain-following coordinates: formulation and skill assessment of the regional Ocean modeling system. J. Comput. Phys. 227 (7), 3595–3624. https://doi.org/10.1016/j.jcp.2007.06.016.
Hallam, S., McCarthy, G.D., Feng, X., Josey, S.A., Harris, E., Düsterhus, A., Ogungbenro, S., Hirschi, J.J.-M., 2023. The relationship between sea surface temperature anomalies, wind and translation speed and North Atlantic tropical cyclone rainfall over ocean and land. Environmental Research Communications 5 (2), 025007. https://doi.org/10.1088/2515-7620/acb31c.
Hersbach, H., Bell, B., Berrisford, P., Hirahara, S., Horányi, A., Muñoz-Sabater, J., Nicolas, J., Peubey, C., Radu, R., Schepers, D., Simmons, A., Soci, C., Abdalla, S., Abellan, X., Balsamo, G., Bechtold, P., Biavati, G., Bidlot, J., Bonavita, M., et al., 2020. The ERA5 global reanalysis. Q. J. R. Meteorol. Soc. 146 (730), 1999–2049. https://doi.org/10.1002/qj.3803.
Hsu, W.-C., Patricola, C.M., Chang, P., 2019. The impact of climate model sea surface temperature biases on tropical cyclone simulations. Clim. Dynam. 53 (1–2), 173–192. https://doi.org/10.1007/s00382-018-4577-5.
Huang, H., Patricola, C.M., Collins, W.D., 2021. The influence of ocean coupling on simulated and projected tropical cyclone precipitation in the HighResMIP–PRIMAVERA simulations. Geophys. Res. Lett. 48 (20) https://doi.org/10.1029/2021GL094801.
Huang, P., Lin, I.-I., Chou, C., Huang, R.-H., 2015. Change in ocean subsurface environment to suppress tropical cyclone intensification under global warming. Nat. Commun. 6 (1), 7188. https://doi.org/10.1038/ncomms8188.
Jacob, R., Larson, J., Ong, E., 2005. M × N communication and parallel interpolation in community climate system model version 3 using the model coupling Toolkit. Int. J. High Perform. Comput. Appl. 19 (3), 293–307. https://doi.org/10.1177/1094342005056116.
Kain, J.S., 2004. The kain–fritsch convective parameterization: an update. J. Appl. Meteorol. 43 (1), 170–181. https://doi.org/10.1175/1520-0450(2004)043<0170:TKCPAU>2.0.CO;2.
Karnauskas, K.B., Zhang, L., Emanuel, K.A., 2021. The feedback of cold wakes on tropical cyclones. Geophys. Res. Lett. 48 (7) https://doi.org/10.1029/2020GL091676.
Kelly, P., Leung, L.R., Balaguru, K., Xu, W., Mapes, B., Soden, B., 2018. Shape of Atlantic tropical cyclone tracks and the Indian monsoon. Geophys. Res. Lett. 45 (19) https://doi.org/10.1029/2018GL080098.
Klotzbach, P.J., 2006. Trends in global tropical cyclone activity over the past twenty years (1986-2005). Geophys. Res. Lett. 33 (10) https://doi.org/10.1029/2006GL025881 n/a-n/a.
Knapp, K.R., Kruk, M.C., Levinson, D.H., Diamond, H.J., Neumann, C.J., 2010. The international best track archive for climate stewardship (IBTrACS). Bull. Am. Meteorol. Soc. 91 (3), 363–376. https://doi.org/10.1175/2009BAMS2755.1.
Knutson, T.R., Camargo, S.J., Chan, J.C.L., Emanuel, K., Ho, C.H., Kossin, J., Mohapatra, M., Satoh, M., Sugi, M., Walsh, K., Wu, L., 2020. Tropical cyclones and climate change assessment part II: projected response to anthropogenic warming. Bull. Am. Meteorol. Soc. 101 (3), E303–E322. https://doi.org/10.1175/BAMS-D-18-0194.1.
Knutson, T.R., McBride, J.L., Chan, J., Emanuel, K., Holland, G., Landsea, C., Held, I., Kossin, J.P., Srivastava, A.K., Sugi, M., 2010. Tropical cyclones and climate change. Nat. Geosci. 3 (3), 157–163. https://doi.org/10.1038/ngeo779.
Knutson, T.R., Sirutis, J.J., Vecchi, G.A., Garner, S., Zhao, M., Kim, H.-S., Bender, M., Tuleya, R.E., Held, I.M., Villarini, G., 2013. Dynamical downscaling projections of twenty-first-century Atlantic hurricane activity: CMIP3 and CMIP5 model-based scenarios. J. Clim. 26 (17), 6591–6617. https://doi.org/10.1175/JCLI-D-12-00539.1.
Knutson, T.R., Sirutis, J.J., Zhao, M., Tuleya, R.E., Bender, M., Vecchi, G.A., Villarini, G., Chavas, D., 2015. Global projections of intense tropical cyclone activity for the late twenty-first century from dynamical downscaling of CMIP5/RCP4.5 scenarios. J. Clim. 28 (18), 7203–7224. https://doi.org/10.1175/JCLI-D-15-0129.1.
Kuttippurath, J., Akhila, R.S., Martin, M.V., Girishkumar, M.S., Mohapatra, M., Balan Sarojini, B., Mogensen, K., Sunanda, N., Chakraborty, A., 2022. Tropical cyclone-induced cold wakes in the northeast Indian Ocean. Environ. Sci. J. Integr. Environ. Res.: Atmosphere 2 (3), 404–415. https://doi.org/10.1039/D1EA00066G.
Lackmann, G.M., 2015. Hurricane sandy before 1900 and after 2100. Bull. Am. Meteorol. Soc. 96 (4), 547–560. https://doi.org/10.1175/BAMS-D-14-00123.1.
Landsea, C.W., Franklin, J.L., 2013. Atlantic hurricane database uncertainty and presentation of a new database format. Mon. Weather Rev. 141 (10), 3576–3592. https://doi.org/10.1175/MWR-D-12-00254.1.
Larson, J., Jacob, R., Ong, E., 2005. The model coupling Toolkit: a new Fortran90 Toolkit for building multiphysics parallel coupled models. Int. J. High Perform. Comput. Appl. 19 (3), 277–292. https://doi.org/10.1177/1094342005056115.
Lau, W.K.M., Zhou, Y.P., 2012. Observed recent trends in tropical cyclone rainfall over the North Atlantic and the North Pacific. J. Geophys. Res. Atmos. 117 (D3) https://doi.org/10.1029/2011JD016510 n/a-n/a.
Li, H., Sriver, R.L., 2018. Tropical cyclone activity in the high-resolution community earth system model and the impact of ocean coupling. J. Adv. Model. Earth Syst. 10 (1), 165–186. https://doi.org/10.1002/2017MS001199.
Li, H., Sriver, R.L., 2019. Impact of air–sea coupling on the simulated global tropical cyclone activity in the high-resolution Community Earth System Model (CESM). Clim. Dynam. 53 (7–8), 3731–3750. https://doi.org/10.1007/s00382-019-04739-8.
Lin, I.-I., Pun, I.-F., Wu, C.-C., 2009. Upper-Ocean thermal structure and the western North pacific category 5 typhoons. Part II: dependence on translation speed. Mon. Weather Rev. 137 (11), 3744–3757. https://doi.org/10.1175/2009MWR2713.1.
Lin, I.-I., Wu, C.-C., Pun, I.-F., Ko, D.-S., 2008. Upper-Ocean thermal structure and the western North pacific category 5 typhoons. Part I: ocean features and the category 5 typhoons' intensification. Mon. Weather Rev. 136 (9), 3288–3306. https://doi.org/10.1175/2008MWR2277.1.
Liu, M., Vecchi, G.A., Smith, J.A., Knutson, T.R., 2019. Causes of large projected increases in hurricane precipitation rates with global warming. Npj Climate and Atmospheric Science 2 (1), 38. https://doi.org/10.1038/s41612-019-0095-3.
Lu, Z., Wang, G., Shang, X., 2021. Inner-core sea surface cooling induced by a moving tropical cyclone. J. Phys. Oceanogr. https://doi.org/10.1175/JPO-D-21-0102.1.
Ma, Z., Fei, J., Lin, Y., Huang, X., 2020. Modulation of clouds and rainfall by tropical cyclone's cold wakes. Geophys. Res. Lett. 47 (17) https://doi.org/10.1029/2020GL088873.
Matyas, C.J., 2013. Processes influencing rain-field growth and decay after tropical cyclone landfall in the United States. J. Appl. Meteorol. Climatol. 52 (5), 1085–1096. https://doi.org/10.1175/JAMC-D-12-0153.1.
Mei, W., Lien, C.-C., Lin, I.-I., Xie, S.-P., 2015a. Tropical cyclone–induced ocean response: a comparative study of the south China sea and tropical northwest Pacific*,+. J. Clim. 28 (15), 5952–5968. https://doi.org/10.1175/JCLI-D-14-00651.1.
Mei, W., Pasquero, C., Primeau, F., 2012. The effect of translation speed upon the intensity of tropical cyclones over the tropical ocean. Geophys. Res. Lett. 39 (7) https://doi.org/10.1029/2011GL050765 n/a-n/a.
Mei, W., Primeau, F., McWilliams, J.C., Pasquero, C., 2013. Sea surface height evidence for long-term warming effects of tropical cyclones on the ocean. Proc. Natl. Acad. Sci. USA 110 (38), 15207–15210. https://doi.org/10.1073/pnas.1306753110.
Mei, W., Xie, S.-P., Primeau, F., McWilliams, J.C., Pasquero, C., 2015b. Northwestern Pacific typhoon intensity controlled by changes in ocean temperatures. Sci. Adv. 1 (4) https://doi.org/10.1126/sciadv.1500014.
Meinshausen, M., Nicholls, Z.R.J., Lewis, J., Gidden, M.J., Vogel, E., Freund, M., Beyerle, U., Gessner, C., Nauels, A., Bauer, N., Canadell, J.G., Daniel, J.S., John, A., Krummel, P.B., Luderer, G., Meinshausen, N., Montzka, S.A., Rayner, P.J., Reimann, S., et al., 2020. The shared socio-economic pathway (SSP) greenhouse gas concentrations and their extensions to 2500. Geosci. Model Dev. (GMD) 13 (8), 3571–3605. https://doi.org/10.5194/gmd-13-3571-2020.
Mogensen, K.S., Magnusson, L., Bidlot, J., 2017. Tropical cyclone sensitivity to ocean coupling in the ECMWF coupled model. J. Geophys. Res.: Oceans 122 (5), 4392–4412. https://doi.org/10.1002/2017JC012753.
NOAA National Centers for Environmental Information (NCEI), 2023. U.S. Billion-Dollar Weather and Climate Disasters. https://doi.org/10.25921/stkw-7w73. April 14).
Pall, P., Patricola, C.M., Wehner, M.F., Stone, D.A., Paciorek, C.J., Collins, W.D., 2017. Diagnosing conditional anthropogenic contributions to heavy Colorado rainfall in September 2013. Weather Clim. Extrem. 17, 1–6. https://doi.org/10.1016/j.wace.2017.03.004.
Pasquero, C., Desbiolles, F., Meroni, A.N., 2021. Air-Sea interactions in the cold wakes of tropical cyclones. Geophys. Res. Lett. 48 (2) https://doi.org/10.1029/2020GL091185.
Patricola, C.M., Wehner, M.F., 2018. Anthropogenic influences on major tropical cyclone events. Nature 563 (7731), 339–346. https://doi.org/10.1038/s41586-018-0673-2.

Price, J.F., 1981. Upper Ocean response to a hurricane. J. Phys. Oceanogr. 11 (2), 153–175. https://doi.org/10.1175/1520-0485(1981)011<0153:UORTAH>2.0.CO;2.

Pun, I., Knaff, J.A., Sampson, C.R., 2021. Uncertainty of tropical cyclone wind radii on sea surface temperature cooling. J. Geophys. Res. Atmos. 126 (14) https://doi.org/10.1029/2021JD034857.

Reed, K.A., Stansfield, A.M., Wehner, M.F., Zarzycki, C.M., 2020. Forecasted attribution of the human influence on Hurricane Florence. Sci. Adv. 6 (1) https://doi.org/10.1126/sciadv.aaw9253.

Riahi, K., van Vuuren, D.P., Kriegler, E., Edmonds, J., O'Neill, B.C., Fujimori, S., Bauer, N., Calvin, K., Dellink, R., Fricko, O., Lutz, W., Popp, A., Cuaresma, J.C., KC, S., Leimbach, M., Jiang, L., Kram, T., Rao, S., Emmerling, J., et al., 2017. The Shared Socioeconomic Pathways and their energy, land use, and greenhouse gas emissions implications: an overview. Global Environ. Change 42, 153–168. https://doi.org/10.1016/j.gloenvcha.2016.05.009.

Richter, I., 2015. Climate model biases in the eastern tropical oceans: causes, impacts and ways forward. WIREs Climate Change 6 (3), 345–358. https://doi.org/10.1002/wcc.338.

Roberts, M.J., Camp, J., Seddon, J., Vidale, P.L., Hodges, K., Vannière, B., Mecking, J., Haarsma, R., Bellucci, A., Scoccimarro, E., Caron, L., Chauvin, F., Terray, L., Valcke, S., Moine, M., Putrasahan, D., Roberts, C.D., Senan, R., Zarzycki, C., et al., 2020. Projected future changes in tropical cyclones using the CMIP6 HighResMIP multimodel ensemble. Geophys. Res. Lett. 47 (14) https://doi.org/10.1029/2020GL088662.

Rotunno, R., Emanuel, K.A., 1987. An air–sea interaction theory for tropical cyclones. Part II: evolutionary study using a nonhydrostatic axisymmetric numerical model. J. Atmos. Sci. 44 (3), 542–561. https://doi.org/10.1175/1520-0469(1987)044<0542:AAITFT>2.0.CO;2.

Schär, C., Frei, C., Lüthi, D., Davies, H.C., 1996. Surrogate climate-change scenarios for regional climate models. Geophys. Res. Lett. 23 (6), 669–672. https://doi.org/10.1029/96GL00265.

Schwinger, J., Tjiputra, J.F., Heinze, C., Bopp, L., Christian, J.R., Gehlen, M., Ilyina, T., Jones, C.D., Salas-Mélia, D., Segschneider, J., Séférian, R., Totterdell, I., 2014. Nonlinearity of ocean carbon cycle feedbacks in CMIP5 earth system models. J. Clim. 27 (11), 3869–3888. https://doi.org/10.1175/JCLI-D-13-00452.1.

Shchepetkin, A.F., McWilliams, J.C., 2005. The regional oceanic modeling system (ROMS): a split-explicit, free-surface, topography-following-coordinate oceanic model. Ocean Model. 9 (4), 347–404. https://doi.org/10.1016/j.ocemod.2004.08.002.

Skamarock, W.C., Klemp, J.B., Dudhia, J., Gill, D.O., Liu, Z., Berner, J., Wang, W., Powers, J.G., Duda, M.G., Barker, D.M., Huang, X.-Y., 2019. *A Description Of the Advanced Research WRF Model Version 4*. NCAR Technical Note (No. NCAR/TN-556+STR). https://doi.org/10.5065/1dfh-6p97.

Srinivas, C.V., Mohan, G.M., Naidu, C.V., Baskaran, R., Venkatraman, B., 2016. Impact of air-sea coupling on the simulation of tropical cyclones in the North Indian Ocean using a simple 3-D ocean model coupled to ARW. J. Geophys. Res. Atmos. 121 (16), 9400–9421. https://doi.org/10.1002/2015JD024431.

Trenberth, K.E., Cheng, L., Jacobs, P., Zhang, Y., Fasullo, J., 2018. Hurricane Harvey links to ocean heat content and climate change adaptation. Earth's Future 6 (5), 730–744. https://doi.org/10.1029/2018EF000825.

Trenberth, K.E., Davis, C.A., Fasullo, J., 2007. Water and energy budgets of hurricanes: case studies of Ivan and Katrina. J. Geophys. Res. 112 (D23), D23106 https://doi.org/10.1029/2006JD008303.

Vial, J., Dufresne, J.-L., Bony, S., 2013. On the interpretation of inter-model spread in CMIP5 climate sensitivity estimates. Clim. Dynam. 41 (11–12), 3339–3362. https://doi.org/10.1007/s00382-013-1725-9.

Villarini, G., Lavers, D.A., Scoccimarro, E., Zhao, M., Wehner, M.F., Vecchi, G.A., Knutson, T.R., Reed, K.A., 2014. Sensitivity of tropical cyclone rainfall to idealized global-scale forcings. J. Clim. 27 (12), 4622–4641. https://doi.org/10.1175/JCLI-D-13-00780.1.

Vincent, E.M., Lengaigne, M., Madec, G., Vialard, J., Samson, G., Jourdain, N.C., Menkes, C.E., Jullien, S., 2012. Processes setting the characteristics of sea surface cooling induced by tropical cyclones. J. Geophys. Res.: Oceans 117 (C2). https://doi.org/10.1029/2011JC007396 n/a-n/a.

Walker, N.D., Leben, R.R., Pilley, C.T., Shannon, M., Herndon, D.C., Pun, I.-F., Lin, I.-I., Gentemann, C.L., 2014. Slow translation speed causes rapid collapse of northeast Pacific Hurricane Kenneth over cold core eddy. Geophys. Res. Lett. 41 (21), 7595–7601. https://doi.org/10.1002/2014GL061584.

Walsh, K.J.E., McBride, J.L., Klotzbach, P.J., Balachandran, S., Camargo, S.J., Holland, G., Knutson, T.R., Kossin, J.P., Lee, T., Sobel, A., Sugi, M., 2016. Tropical cyclones and climate change. WIREs Climate Change 7 (1), 65–89. https://doi.org/10.1002/wcc.371.

Warner, J.C., Armstrong, B., He, R., Zambon, J.B., 2010. Development of a Coupled OceanOcean–Atmosphere–Wave–sediment Transport (COAWST) modeling system. Ocean Model. 35 (3), 230–244. https://doi.org/10.1016/j.ocemod.2010.07.010.

Wehner, M.F., Zarzycki, C., Patricola, C., 2019. Estimating the Human Influence on Tropical Cyclone Intensity as the Climate Changes, pp. 235–260. https://doi.org/10.1007/978-3-030-02402-4_12.

Wright, D.B., Knutson, T.R., Smith, J.A., 2015. Regional climate model projections of rainfall from U.S. landfalling tropical cyclones. Clim. Dynam. 45 (11–12), 3365–3379. https://doi.org/10.1007/s00382-015-2544-y.

Wu, L., Wang, B., Braun, S.A., 2005. Impacts of air–sea interaction on tropical cyclone track and intensity. Mon. Weather Rev. 133 (11), 3299–3314. https://doi.org/10.1175/MWR3030.1.

Zarzycki, C.M., 2016. Tropical cyclone intensity errors associated with lack of two-way ocean coupling in high-resolution global simulations. J. Clim. 29 (23), 8589–8610. https://doi.org/10.1175/JCLI-D-16-0273.1.

Zhang, J., Lin, Y., Chavas, D.R., Mei, W., 2019. Tropical cyclone cold wake size and its applications to power dissipation and ocean heat uptake estimates. Geophys. Res. Lett. 46 (16), 10177–10185. https://doi.org/10.1029/2019GL083783.

Zhang, G., Murakami, H., Yang, X., Findell, K.L., Wittenberg, A.T., Jia, L., 2021a. Dynamical seasonal predictions of tropical cyclone activity: roles of sea surface temperature errors and atmosphere–land initialization. J. Clim. 34 (5), 1743–1766. https://doi.org/10.1175/JCLI-D-20-0215.1.

Zhang, H., He, H., Zhang, W.-Z., Tian, D., 2021b. Upper ocean response to tropical cyclones: a review. Geoscience Letters 8 (1), 1. https://doi.org/10.1186/s40562-020-00170-8.

Zuidema, P., Chang, P., Medeiros, B., Kirtman, B.P., Mechoso, R., Schneider, E.K., Toniazzo, T., Richter, I., Small, R.J., Bellomo, K., Brandt, P., de Szoeke, S., Farrar, J. T., Jung, E., Kato, S., Li, M., Patricola, C., Wang, Z., Wood, R., Xu, Z., 2016. Challenges and prospects for reducing coupled climate model SST biases in the eastern tropical Atlantic and pacific oceans: the U.S. CLIVAR eastern tropical oceans synthesis working group. Bull. Am. Meteorol. Soc. 97 (12), 2305–2328. https://doi.org/10.1175/BAMS-D-15-00274.1.